bline coupler can be accurately predicted by the Bloch-wave analysis, in spite of its very complicated topology. To find the curves in Fig. 11 parasitic effects such as stray coupling capacitances at the strip open ends were accounted for by static methods. Minor discrepancies can probably be ascribed to the imperfect behavior of the terminations used to carry out the measurements [11]. The excellent accuracy of the Bloch-wave results shown in Fig. 11 is especially interesting in view of the fact that no alternative approach based on sound physical arguments is available to date for analyzing such devices.

References

[1] D. J. Gunton and E. G. S. Paige, "Directional coupler for gigahertz frequencies based on the coupling properties of two planar comb transmission lines," *Electron. Lett.*, vol. 11, pp. 406–408, 1975.

[2] D. J. Gunton, "Design of wideband codirectional couplers and their realization at microwave frequencies using coupled comblines," *IEE J. Microwaves, Opt., Acoust.*, vol. 2, pp. 19–30, 1978.

[3] J. T. Bolljahn and G. L. Matthaei, "A study of the phase and filter properties of arrays of parallel conductors between ground planes," *Proc. IRE*, vol. 50, pp. 299–311, 1962.

[4] R. Pregla, "Meander lines for delay equalization," in *Proc. Conf. Trunk Telecommunications by Guided Waves*, IEE Conf. Pub. N. 71, Sept. 1970, pp. 171–175.

[5] J. A. Weiss, "Dispersion and field analysis of a microstrip meander-line slow-wave structure," *IEEE Trans. Microwave Theory Tech.*, vol. MTT-22, pp. 1194–1201, Dec. 1974.

[6] J. I. Smith, "The even- and odd-mode capacitance parameters for coupled lines in suspended substrate," *IEEE Trans. Microwave Theory Tech.*, vol. MTT-19, pp. 424–431, May 1971.

[7] G. I. Zysman and A. K. Johnson, "Coupled transmission line networks in an inhomogeneous dielectric medium," *IEEE Trans. Microwave Theory Tech.*, vol. MTT-17, pp. 753–759, Oct. 1969.

[8] V. A. Monaco and P. Tiberio, "Computer-aided analysis of microwave circuits," *IEEE Trans. Microwave Theory Tech.*, vol. MTT-22, pp. 249–263, Mar. 1974.

[9] V. Rizzoli and A. Lipparini, "Coupled combline structures for use in M.I.C.'s," in *Proc. 8th European Microwave Conf.*, (Paris, France), Sept. 1978, pp. 84–88.

[10] R. E. Collin, *Foundation for Microwave Engineering*. New York: Mc-Graw Hill, 1966, pp. 369–390.

[11] V. Rizzoli and A. Lipparini, "A graphical approach to the design of multistrip components for M.I.C.'s," in *Proc. Int. Conf. Interactive Techniques in Computer-aided Design*, (Bologna, Italy), Sept. 1978, pp. 296–302.

Analysis of Small Aperture Coupling Between Rectangular Waveguide and Microstrip Line

J. S. RAO, K. K. JOSHI, AND B. N. DAS

***Abstract*—This paper presents a generalized analysis on aperture coupling between a microstripline and a rectangular waveguide. The orthonormalized modal functions for the microstrip line required for the determination of the equivalent dipole moment are found from its equivalent parallel plate configuration. Expressions for coupling are obtained for transmission lines with their axes parallel, the lines forming a T-junction and also for cross-guide couplers. Theoretical results show good agreement with the experimental data for all cases under investigation.**

I. Introduction

IN ORDER to integrate waveguide circuitry with strip and microstrip circuitry, it is essential to realize coupling between these dissimilar lines. Some studies on the aperture coupling between a waveguide and a strip or a microstrip line with their axes parallel have been reported in the literature [1]–[4]. The coupling coefficient has been defined in the published literature as the ratio of the voltage in the coupled line to that in the primary line. The expressions obtained do not, however, exhibit reciprocal properties of the device.

Manuscript received June 9, 1980; revised September 30, 1980.

The authors are with the Department of Electronics and Electrical Communication Engineering, Indian Institute of Technology, Kharagpur-721302, India.

In the present work the coupling between dissimilar guides is expressed as the ratio of the power flowing down the coupled guide to that in the primary guide. If the generator and coupled ports are designated as 1 and 2, respectively, the power coupling coefficients are the same for the directions $1 \rightarrow 2$ and $2 \rightarrow 1$. The expression for the power flow in a line is obtained from the product of the square of the model voltage [8] and the wave admittance of the propagating mode. For a TEM mode line the ratio of the modal voltage to modal current is equal to the wave admittance [7].

Analysis of aperture coupling between the rectangular waveguide and the microstrip line is restricted to small aperture, as the latter is replaced by its dipole moments [5], [6]. Amplitude of the modal voltage of the wave propagating in the coupled guide is determined from a knowledge of the equivalent dipole moment of the aperture and the orthonormalized field functions [8] in the coupled

0018-9480/81/0200-0150$00.75

guide. In the case of microstrip line, the eigenfunctions required for the analysis are obtained from its equivalent parallel plate configuration [9].

Expressions for power coupling coefficients are derived for the following cases: 1) rectangular waveguide and microstripline with their axes parallel; 2) rectangular waveguide and microstrip line forming a T-junction; and 3) crossed waveguide and microstripline couplers. Comparison between theoretical and experimental results for small apertures in the forms of narrow rectangular slots and circular holes are presented.

II. Coupling Between Parallel Rectangular Waveguide and Microstrip Line Through Apertures in the Common Wall

Consider a rectangular waveguide coupled to a microstrip line through an aperture centrally located in the common ground plane as shown in Fig. 1(a). The electric and magnetic fields in the guides are expressed in terms of modal vector $\boldsymbol{e}$ and modal voltage v, and modal vector $\boldsymbol{h}$ and modal current I, respectively, [8]. The orthogonal modal vectors $\boldsymbol{e}$ and $\boldsymbol{h}$ satisfy the normalization condition

$$\int\int \boldsymbol{e}\cdot\boldsymbol{e}\,ds=\int\int \boldsymbol{h}\cdot\boldsymbol{h}\,ds=1.$$

The normalized modal vectors for the dominant TE_{10} mode in the rectangular waveguide are given by [8]

$$\boldsymbol{e}_1=\sqrt{\frac{2}{ab}}\;\boldsymbol{U}_Y\cos\frac{\pi x}{a}\,e^{-j\beta_{10}z} \tag{1}$$

$$\boldsymbol{h}_1=\sqrt{\frac{2}{ab}}\left[-\boldsymbol{U}_x\cos\frac{\pi x}{a}+\frac{j\pi}{\beta_{10}a}\boldsymbol{U}_z\sin\frac{\pi x}{a}\right]e^{-j\beta_{10}z}. \tag{2}$$

The normalized electric and magnetic fields are of the form

$$\boldsymbol{E}_1=v_1\boldsymbol{e}_1 \tag{2a}$$

$$\boldsymbol{H}_1=I_1\boldsymbol{h}_1=y_{10}v_1\boldsymbol{h}_1 \tag{2b}$$

where v_1 and I_1 are, respectively, the effective values of modal voltage and modal current and y_{10} is the characteristic wave admittance. The power carried by this wave is given by

$$P_1=y_{10}v_1^2. \tag{3}$$

The normalized eigenfunctions for a microstrip line are determined from its equivalence to a parallel plate line. It has been established that the microstrip line of strip width shown in Fig. 1(a) is equivalent to the parallel plate line shown in Fig. 1(b) such that the effective width D of the parallel plate line is given by [9]

$$D=\frac{h}{Z_0}\frac{120\pi}{\sqrt{\epsilon_{r\text{eff}}}} \tag{4}$$

where the effective dielectric constant of the equivalent parallel plate line is given by

$$\sqrt{\epsilon_{r\text{eff}}}=\left[\frac{\epsilon_r+1}{2}+\left(\frac{\epsilon_r-1}{2}\right)\left(1+10\frac{h}{d}\right)^{-1/2}\right]^{1/2}. \tag{5}$$

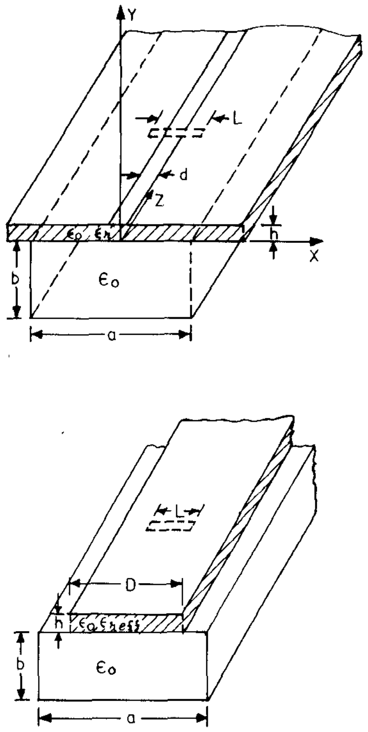

Fig. 1. (a) Aperture coupling between microstrip and rectangular waveguide when their axes are parallel. (b) The coupler of (a) with microstrip replaced by its equivalent parallel plate guide.

The height h of the parallel plate line is equal to the thickness ($h=1/16''$) of the microstrip substrate. The normalized modal vectors for the TEM mode in the parallel plate line shown in Fig. 1(b) are obtained as [8]

$$\boldsymbol{e}_2=\boldsymbol{U}_y\sqrt{\frac{1}{Dh}}\;e^{-j\beta z} \tag{6a}$$

$$\boldsymbol{h}_2=-\boldsymbol{U}_x\sqrt{\frac{1}{Dh}}\;e^{-j\beta z}. \tag{6b}$$

The corresponding electric and magnetic fields are given by

$$\boldsymbol{E}_2=v_2\boldsymbol{e}_2 \tag{7a}$$

$$\boldsymbol{H}_2=I_2\boldsymbol{h}_2=y_0v_2\boldsymbol{h}_2 \tag{7b}$$

where v_2 and I_2 are, respectively, the effective values of modal voltage and current of the TEM mode and y_0 ($=\sqrt{\epsilon_{r\text{eff}}}/120\pi$) is the characteristic wave admittance. The power carried by this mode is given by

$$P_2=y_0v_2^2. \tag{8}$$

For a generator connected to the rectangular waveguide of Fig. 1 at $z=-\alpha$, the aperture in the common wall can be replaced by its equivalent electric and magnetic dipoles which radiate towards $z>0$ as well as $z<0$ in both the guides. The equivalent electric and magnetic dipole moments $\boldsymbol{P}$ and $\boldsymbol{M}$, respectively, are given by [7]

$$\boldsymbol{P}=-\alpha_e\boldsymbol{nn}\cdot\boldsymbol{E}_n \tag{9a}$$

$$\boldsymbol{M}=-\bar{\bar{\alpha}}_m\cdot\boldsymbol{H}_t \tag{9b}$$

where $\boldsymbol{E}_n$ and $\boldsymbol{H}_t$ are normal electric and tangential magnetic fields in the primary guide at the aperture. α_e is the electric polarizability of the aperture and $\bar{\bar{\alpha}}_m$ is the dyadic magnetic polarizability of the aperture which is given by

$$\bar{\bar{\alpha}}_m = \alpha_{mx}(\boldsymbol{U}_x\boldsymbol{U}_x) + \alpha_{mz}(\boldsymbol{U}_z\boldsymbol{U}_z). \tag{10}$$

The modal voltage of the TEM mode wave traveling in the forward and backward directions due to the radiation from the electric and magnetic dipoles, in the coupled line, are obtained as [10]

$$v_2^+ = -\boldsymbol{U}_y\sqrt{\frac{1}{Dh}}\,\frac{1}{2y_0}\cdot(-jw\epsilon\alpha_e\boldsymbol{U}_y\boldsymbol{U}_y\cdot\boldsymbol{E}_1) + \frac{jw\mu_0}{2y_0}\left(\boldsymbol{U}_x y_0\sqrt{\frac{1}{Dh}}\right)\cdot\left(-\bar{\bar{\alpha}}_m\cdot\boldsymbol{H}_1\right) \tag{11a}$$

and

$$v_2^- = -\boldsymbol{U}_y\sqrt{\frac{1}{Dh}}\,\frac{1}{2y_0}\cdot(-jw\epsilon\alpha_e\boldsymbol{U}_y\boldsymbol{U}_y\cdot\boldsymbol{E}_1) + \frac{jw\mu_0}{2y_0}\left(-\boldsymbol{U}_x y_0\sqrt{\frac{1}{Dh}}\right)\cdot\left(-\bar{\bar{\alpha}}_m\cdot\boldsymbol{H}_1\right). \tag{11b}$$

From (8) the power coupled in the forward and backward direction is given by

$$P_2^+ = |v_2^+|^2 y_0 \tag{12a}$$

and

$$P_2^- = |v_2^-|^2 y_0. \tag{12b}$$

The coupling in the forward and in the reverse directions are obtained as

$$C^+(\text{dB}) = 10\log_{10}(P_2^+/P_1) \tag{13a}$$

and

$$C^-(\text{dB}) = 10\log_{10}(P_2^-/P_1). \tag{13b}$$

The above general formulation will be used for the calculation of coupling through apertures in the form of thin rectangular slots and circular holes. For an aperture centrally located in the common wall between the two transmission lines, the coupling is obtained from (1) to (3) and (10) to (13) as

$$C^+(\text{dB}) = 10\log_{10} \cdot\left[\frac{2}{abDh}\left(\frac{w\epsilon\alpha_e}{2\sqrt{y_0y_{10}}} + \frac{w\mu_0\alpha_{mx}}{2}\sqrt{y_0y_{10}}\right)^2\right] \tag{14a}$$

$$C^-(\text{dB}) = 10\log_{10} \cdot\left[\frac{2}{abDh}\left(\frac{w\epsilon\alpha_e}{2\sqrt{y_0y_{10}}} - \frac{w\mu_0\alpha_{mx}}{2}\sqrt{y_0y_{10}}\right)^2\right]. \tag{14b}$$

The above expressions are derived for the equivalent parallel plate configuration of Fig. 1(b). Because of the fact that in Fig. 1(b) there are two different dielectric media on either side of the aperture (air on one side and dielectric medium with relative effective dielectric constant $\epsilon_{r\text{eff}}$ on the other side), the effective dielectric constant ϵ to be used in the above expressions is of the form [11]

$$\epsilon = \frac{\epsilon_0 2\epsilon_{r\text{eff}}}{1+\epsilon_{r\text{eff}}}. \tag{15}$$

A. Case (1)—Centered Rectangular Slot

For thin rectangular slots experimental data on α_e and α_{mx} have been obtained by Cohn [12],[13]. Numerical data on α_e and α_{mx} for identical aperture have also been determined by De Meulenaere and Van Bladel [14].

Using above data on α_e and α_{mx} for thin rectangular slots, coupling is calculated from (4), (5), (14), and (15). Computations are made for $\lambda = 10$ cm, $\epsilon_r = 2.56$ for slot lengths in the range 0.3 cm to 0.8 cm and slot widths of 0.1 cm and 0.2 cm, etched in the ground plane of a 50-Ω microstrip line coupled to a rectangular waveguide having the dimensions $a = 7.2$ cm and $b = 3.4$ cm. For a 50-Ω microstrip line with $h = 1/16'' \approx 0.16$ cm, $d = 0.44$ cm for $\epsilon_r = 2.56$. For this line $D \approx 0.83$ cm and $\epsilon_{r\text{eff}} \approx 2.09$. The computed results on forward and reverse coupling are presented in Fig. 2(a) and 2(b) together with experimental results.

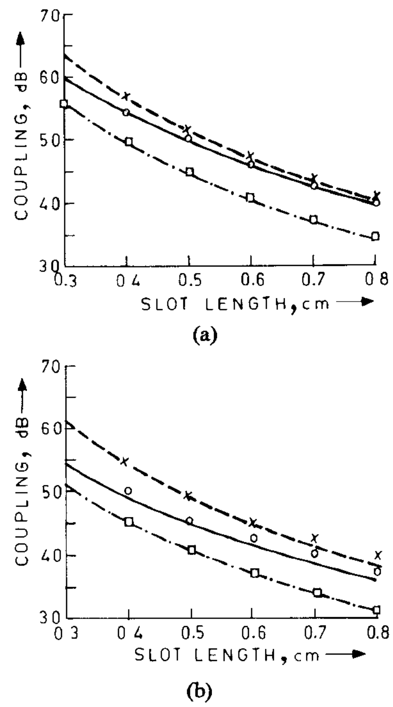

Fig. 2. Variation of coupling with slot length for $\lambda = 10$ cm, $a = 7.2$ cm, $b = 3.4$ cm, $h = 0.16$ cm, $d = 0.44$ cm, $\epsilon_r = 2.56$. (a) Slot width = 0.1 cm. (i) Coupler using transmission lines with their axes parallel. — — — forward coupling (theoretical). × × × forward coupling (experimental). —— reverse coupling (theoretical). ○ ○ ○ Reverse coupling (experimental). (ii) T-junction. — · — · — theoretical. □□□ experimental. (b) Slot width = 0.2 cm. (i) Coupler using transmission lines with their axes parallel. — — — forward coupling (theoretical). × × × forward coupling (experimental). ○ ○ ○ reverse coupling (experimental). —— reverse coupling (theoretical). (ii) T-junction. — · — · — theoretical. □□□ experimental.

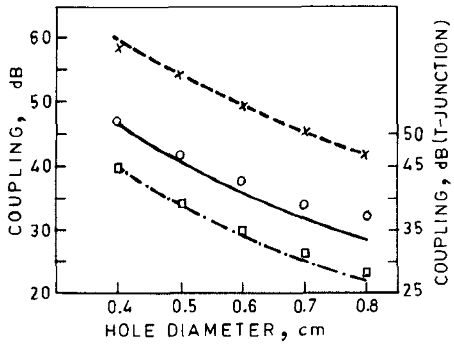

Fig. 3. Variation of coupling with diameter of circular hole for $\lambda = 10$ cm, $a = 7.2$ cm, $b = 3.4$ cm, $h = 0.16$ cm, $d = 0.44$ cm, $\epsilon_r = 2.56$. (i) Coupler using transmission lines with their axes parallel. — — — forward coupling (theoretical). × × × forward coupling (experimental). —— reverse coupling (theoretical). ○○○ reverse coupling (experimental). (ii) T-junction. —·—·— theoretical. □□□ experimental.

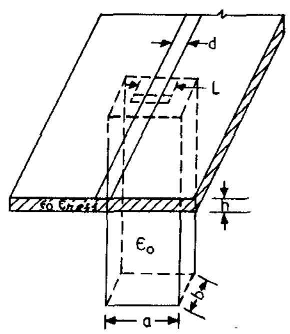

Fig. 4. Microstrip and waveguide forming a T-junction.

B. Case (2)—Centered Circular Hole

The electric and magnetic polarizabilities for a circular hole are calculated from the expressions [10]

$$\alpha_e = -\frac{2}{3} r^3 \tag{16}$$

$$\alpha_{mx} = \frac{4}{3} r^3 \tag{17}$$

where r is the radius of the circular hole. Using (4), (5), and (14)–(17), coupling is calculated for hole diameters in the range 0.4 cm to 0.8 cm at 300-MHz frequency. The computed results are presented in Fig. 3 together with the experimental values.

III. T-Junction Coupler

Consider the structure of Fig. 4. In this case the electric dipole does not have any contribution to the coupling and only the magnetic dipole is responsible for the coupling of the energy from one guide to the other. It is assumed that the generator is connected to the waveguide of Fig. 4. The magnetic field at the center of a small aperture in the cross section of the waveguide is double the incident magnetic field [10]. Modifying the expression (2b) accordingly, and following the procedure of Section II, the expression for the coupling coefficient is obtained as

$$C^+ = C^- = 10\log_{10}\left[\frac{2}{abDh}(w\mu_0\alpha_{mx}y_0y_{10})^2\right]. \tag{18}$$

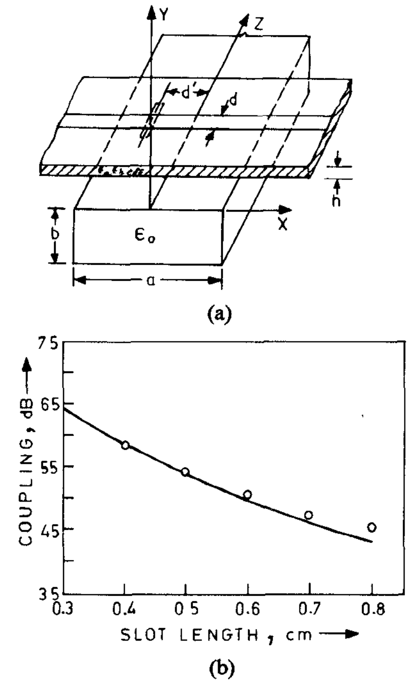

Fig. 5. (a) Crossguide coupler using microstrip and rectangular waveguide. (b) Variation of the coupling with slot length for a cross coupler $\lambda = 10$ cm, $a = 7.2$ cm, $b = 3.4$ cm, $h = 0.16$ cm, $d = 0.44$ cm $\epsilon_r = 2.56$. Slot width $= 0.1$ cm; slot displacement off waveguide axis, $d' = 1.8$ cm. —— theoretical. ○○○ experimental.

Numerical computations are made for apertures in the forms of 1) thin centered transverse slot, and 2) centered circular hole. The dimensions of the apertures and frequency of measurement are the same as those described in Section II. The chain dotted curves in Figs. 2(a), 2(b), and 3 represent the theoretical results for 1) slot of width 1 mm, 2) slot of width 2 mm, and 3) circular hole, respectively. The corresponding experimental results are also presented in these figures for the sake of comparison.

IV. Cross-Guide Coupler

A cross-guide coupler, as shown in Fig. 5(a), is considered. In this case, the coupling slot is so oriented that it is transverse to the axis of the microstripline and is longitudinal and displaced from the axis of the waveguide. Considering the generator to be connected to the rectangular waveguide, the amplitude of the modal voltage induced in the microstrip line due to the electric dipole is given by

$$V_e^+ = V_e^- = \frac{jw\epsilon\alpha_e}{2y_o}\sqrt{\frac{2}{abDh}}\cos\frac{\pi d'}{a} \tag{19}$$

where d' is the displacement of the longitudinal slot from the axis of the waveguide. Amplitude of the modal voltage induced due to the magnetic dipole is obtained as

$$V_m^+ = -V_m^- = \frac{w\mu y_{10}\pi\alpha_{mz}}{2\beta_{10}a}\sqrt{\frac{2}{abDh}}\sin\frac{\pi d'}{a}. \tag{20}$$

Total amplitude of the modal voltage induced in the stripline is the vector sum of v_e and v_m. Thus

$$V_2^+ = V_2^- = \left[\left(\frac{w\epsilon\alpha_e}{2y_0} \sqrt{\frac{2}{abDh}} \cos\frac{\pi d'}{a} \right)^2 + \left(\frac{w\mu y_{10}\pi\alpha_{mz}}{2\beta_{10}a} \sqrt{\frac{2}{abDh}} \sin\frac{\pi d'}{a} \right)^2 \right]^{1/2} \tag{21}$$

and the expression for coupling is obtained as

$$C^+ = C^- = 10\log_{10}\left[\frac{2}{abDh} \left\{ \left(\frac{w\epsilon\alpha_e}{2\sqrt{y_{10}y_0}} \cos\frac{\pi d'}{a} \right)^2 + \left(\frac{w\mu\pi\alpha_{mz}\sqrt{y_0 y_{10}}}{2\beta_{10}a} \sin\frac{\pi d'}{a} \right)^2 \right\} \right]. \tag{22}$$

Numerical computations are made for a slot of width 1 mm and length in the range 0.4 cm to 0.8 cm with displacement $d' = a/4$ from the axis of the waveguide at $\lambda = 10$ cm. The computed results together with the experimental values are presented in Fig. 5(b).

V. Discussion

The analysis presented is based on representation of apertures by dipole moments due to Bethe [5]. This representation is valid for apertures having dimensions small compared to wavelength and locations far from the guide walls [15]. In the case of slots, the data on electric and magnetic polarizabilities used for calculations are valid for relatively large length to width ratio. This accounts for fairly good agreement between theoretical and experimental results on slots presented in Figs. 2, 3, and 5. In the case of circular apertures, however, the discrepancy between the theoretical and experimental results of Figs. 2, 3, and 5 as the diameter of the circle increases, can be attributed to the use of quasi-static formula for dipole moments [5] and to the distortion of the field lines in the vicinity of the aperture as its diameter is increased [15]. The latter is particularly of significance in the case of T-junction, for which a discrepancy of 4 dB between the theoretical and experimental values of reverse coupling is observed at a diameter of 0.8 cm in Fig. 3. Since $D \approx 0.83$ cm, the maximum length of the slot and diameter of circular hole are limited to 0.8 cm.

When the coupled lines under consideration are parallel, the coupling is tighter in the reverse direction which is stronger in the case of coupling through a circular hole as compared to that in the case of transverse slot. Since the copper cladding of the microstripline has a thickness of the order of 30 μm, wall thickness correction is negligible at $\lambda = 10$ cm. The method of analysis is quite general and is applicable not only to parallel coupled lines but also to T-junctions and cross-guide couplers. The results obtained are useful for developing multiaperture directional coupler.

Acknowledgment

The authors wish to thank Dr. V. M. Pandharipande for useful suggestions.

References

[1] H. Perini and P. Sferrazza, "Rectangular waveguide to strip transmission line directional Couplers," in *IRE WESCON Conv. Rec.*, vol. 1, part 1, pp. 16–21, 1957.

[2] W. J. R. Hoefer and D. S. James, "Microstrip to waveguide coupling through holes," in *Proc. 5th Colloquium Microwaves Communication*, (Budapest, Hungary), vol. IV, June 24–30, 1974, pp. 221–231.

[3] M. Kumar and B. N. Das, "Coupled transmission lines," *IEEE Trans. Microwave Theory Tech.*, vol. MTT-25, pp. 7–10, Jan. 1977.

[4] S. N. Prasad and S. Mahapatra, "Waveguide to microstrip multiaperture directional coupler," in *Proc. 9th European Microwave Conf.*, (Brighton, England), Sept. 17–21, 1979, pp. 425–429.

[5] H. A. Bethe, "Theory of diffraction by small holes," *Phys. Rev.*, vol. 66, pp. 163–182, 1944.

[6] S. B. Cohn, "Microwave coupling by large apertures," *Proc. IRE*, vol. 40, pp. 697–699, June 1952.

[7] R. E. Collin, *Field Theory of Guided Waves*. New York: McGraw Hill, 1960.

[8] R. F. Harrington, *Time Harmonic Electromagnetic Fields*. New York: Mc-Graw Hill, 1961.

[9] M. V. Schneider, "Microstriplines for microwave integrated Circuits," *Bell Syst. Tech. J.*, vol. 48, pp. 1421–1445, May/June, 1969.

[10] R. E. Collin, *Foundations for Microwave Engineering*. New York: Mc-Graw Hill, 1966.

[11] J. Van Bladel, "Small hole in a Waveguide wall," *Proc. Inst. Elec. Eng.* vol. 118, pp. 43–50, Jan. 1971.

[12] S. B. Cohn, "Determination of aperture parameters by electrolytic tank measurements," *Proc. IRE*, vol. 39, pp. 1416–1421, Nov. 1951.

[13] S. B. Cohn, "The electric polarisability of apertures of arbitrary shape," *Proc. IRE*, vol. 40, pp. 1069–1071, Sept. 1952.

[14] F. De Meulenaere, and J. Van Bladel, "Polarisability of small apertures," *IEEE Trans. Antennas Propagat.*, vol. AP-25, pp. 198–205, Mar. 1977.

[15] A. A. Oliner, "Equivalent circuits for small symmetrical longitudinal apertures and obstacles," *IEEE Trans., Microwave Theory Tech.*, vol. MTT-9, pp. 72–80, Jan. 1960.